Exosomal Secretion of Cytoplasmic Prostate Cancer Xenograft-derived Proteins*Ⓢ

Flip H. Jansen‡, Jeroen Krijgsveld§, Angelique van Rijswijk‡, Gert-Jan van den Bemd‡, Mirella S. van den Berg‡, Wytske M. van Weerden‡, Rob Willemsen¶, Lennard J. Dekker‖, Theo M. Luider‖, and Guido Jenster‡

**Novel markers for prostate cancer (PCa) are needed because current established markers such as prostate-specific antigen lack diagnostic specificity and prognostic value. Proteomics analysis of serum from mice grafted with human PCa xenografts resulted in the identification of 44 tumor-derived proteins. Besides secreted proteins we identified several cytoplasmic proteins, among which were most subunits of the proteasome. Native gel electrophoresis and sandwich ELISA showed that these subunits are present as proteasome complexes in the serum from xenograft-bearing mice. We hypothesized that the presence of proteasome subunits and other cytoplasmic proteins in serum of xenografted mice could be explained by the secretion of small vesicles by cancer cells, so-called exosomes. Therefore, mass spectrometry and Western blotting analyses of the protein content of exosomes isolated from PCa cell lines was performed. This resulted in the identification of mainly cytoplasmic proteins of which several had previously been identified in the serum of xenografted mice, including proteasome subunits. The isolated exosomes also contained RNA, including the gene fusion *TMPRSS2-ERG* product. These observations suggest that although their function is not clearly defined cancer-derived exosomes offer possibilities for the identification of novel biomarkers for PCa.   *Molecular & Cellular Proteomics 8: 1192–1205, 2009.*

For several decades now, prostate-specific antigen (PSA)[1] has been utilized as the "gold standard" biomarker for the detection of prostate cancer (PCa) (1). Its introduction caused a dramatic decrease in the prevalence of advanced stages of PCa (2). However, ongoing efforts are being made to discover new biomarkers for PCa because it became clear that PSA has limited diagnostic specificity and prognostic value, leading to an enormous increase in unnecessary biopsies and overtreatment of low risk PCa patients (3).

In the last decades, many alternative diagnostic or prognostic markers for PCa have been proposed on protein as well as on RNA and genomic levels. Examples of alternative markers on the protein level are numerous, including various PSA isoforms, prostate stem cell antigen, human kallikrein 2, early prostate cancer antigen, and α-methylacyl-CoA racemase (4–8). On the RNA level, the PCA3 test and especially the recently discovered fusion of TMPRSS2 with ETS transcription factors may hold promise for PCa detection and potentially prognosis in the near future (9, 10). One of the drawbacks of the latter two as markers for PCa is the fact that they are detected in urine, after a standardized prostatic massage, instead of in serum or plasma. This will hamper retrospective validation as most historical biorepositories do not contain urine. Although several validation studies of promising candidates have been performed in the past or are currently underway, no single marker has yet outperformed PSA, justifying ongoing efforts in searching for PCa biomarkers.

One approach is the screening of large series of serum samples from men with and without PCa. However, given the large sample variability, the high complexity, and dynamic range of proteins in serum samples, large numbers of human serum samples have to be analyzed to achieve any statistical significance. Also identified proteins may be related to secondary body defense mechanisms rather than being directly derived from the tumor cells as are most tumor markers applied in the clinic today. To circumvent these problems, we have exploited the xenograft model system as a platform for the discovery of new biomarkers for PCa (11). As has recently been reported, this model system is indeed capable of identifying human proteins that are shed into the circulation by human prostate cancer cells (12).

In the present study we further exploited this approach and performed an in-depth proteomics analysis of serum of mice carrying androgen-sensitive (PC346) or androgen-independent prostate cancer xenografts (PC339). Among the discovered human proteins were numerous cytoplasmic proteins,

[1] The abbreviations used are: PSA, prostate-specific antigen; PCa, prostate cancer; ADAM, a disintegrin and metalloprotease; IPI, International Protein Index; GAPDH, glyceraldehyde-3-phosphate dehydrogenase; LTQ, linear trap quadrupole; HRS, hepatocyte growth factor-regulated tyrosine kinase substrate (also known as HGS); ERG, ETS-related gene; 1D, one-dimensional; VCaP, Vertebral Cancer of the Prostate.

such as glyceraldehyde-3-phosphate dehydrogenase (GAPDH), lactate dehydrogenases A and B, and various subunits of the proteolytic proteasome complex (12). Many of these cytoplasmic proteins are also present in the human plasma proteome as retrieved from the database of the Human Proteome Organisation Plasma Proteome Project (13).

We hypothesized that the presence of cytoplasmic tumor-derived proteins in the xenograft sera could be explained by the secretion of exosomes. Exosomes are small membrane vesicles secreted by virtually every cell type, including tumor cells (14). Exosomes are formed in multivesicular bodies by inward budding, thereby encapsulating cytoplasmic components (14, 15). The exact function of exosomes in tumor cells has yet to be elucidated but is expected to relate to roles in cell-to-cell contact, tumor-stroma interaction, protein degradation, and antigen presentation (14, 15). In addition to containing proteins, it was recently discovered that exosomes also contain functional RNA, proposed as "exosomal shuttle RNA" (16).

To confirm our hypothesis that the cytoplasmic tumor-derived proteins in the serum of xenograft-bearing mice were the result of exosomal secretion, we isolated exosomes from the PC346C cell line and analyzed their protein content. To further explore the contents of exosomes we isolated and analyzed exosomal RNA from both the PC346C and VCaP cell lines.

EXPERIMENTAL PROCEDURES

Xenograft Serum Collection—Human prostate cancer xenografts were grown on immune-incompetent mice athymic male nude (nu/nu) BALB/c mice ($n = 9$ for each xenograft; Taconic, Ry, Denmark) (11, 12). We used the human prostate cancer cell lines PC346 (androgen-sensitive) and PC339 (androgen-independent). Specific characteristics have been described previously (17). Prior control serum was collected by retro-orbital punction. Tumor-bearing mice were sacrificed after 4–5 weeks, and blood was collected. Samples were stored at -80 °C. The protocol was approved by the Animal Experiments Committee under the national Experiments on Animals Act and adhered to the rules laid down in this national law that serves the implementation of "Guidelines on the protection of experimental animals" by the council of Europe under Directive 86/609/EC.

Preparation of Xenograft Sera for Mass Spectrometry—After filtration using a 0.22-μm spin filter, high abundance proteins were removed utilizing Multi Affinity Removal Spin cartridges (Agilent Technologies, Wilmington, DE) according to the manufacturer's instructions. Depleted samples were concentrated on 5-kDa-cutoff ultracentrifugation columns (Agilent Technologies). Total protein concentration was determined by the Bradford method (Bio-Rad). Precast 4–20% polyacrylamide linear gradient gels (Bio-Rad) were utilized to separate 10 μg of protein of depleted mouse serum (pooled from nine individual control mice, nine PC339 xenograft-bearing mice, or nine PC346 xenograft-bearing mice) by SDS-PAGE (Mini-Protean III, Bio-Rad). Prestained high range molecular weight markers (See-Blue, Invitrogen) were loaded on each gel. After running, gels were stained by Coomassie Brilliant Blue (Merck).

Gel lanes (range, 5–200 kDa) were excised and divided into 3-mm sections. Gel slices were washed, destained twice (50% (v/v) acetonitrile in 50 mM ammonium bicarbonate), dehydrated (100% acetonitrile), and reduced with 6.5 mM DTT in 50 mM ammonium bicarbonate for 1 h at 37 °C. After alkylation with 54 mM iodoacetamide in 50 mM

ammonium bicarbonate, proteins were dehydrated in 100% acetonitrile and then rehydrated with the digestion solution containing 10 ng/μl ultra grade sequencing trypsin (Promega, Madison, WI) for 30 min at room temperature. After addition of 30 μl of 50 mM ammonium bicarbonate solution, gel particles were incubated overnight at 37 °C. The peptides were extracted using 0.5% formic acid in 50% acetonitrile, dried completely in a vacuum centrifuge, and stored at -80 °C until analysis.

Liquid Chromatography-Mass Spectrometry of Xenograft Sera—Nanoflow LC-tandem mass spectrometry was performed for samples by coupling an Agilent 1100 HPLC system (Agilent Technologies), operated as described previously (12), to a 7-tesla LTQ-FT mass spectrometer (FT-ICR-MS, Thermo Electron, Bremen, Germany). For protein identification, database searches were performed using Mascot version 2.0 (Matrix Science, London, UK) allowing 5-ppm mass deviation for the precursor ion, a 0.6-Da tolerance on the fragment ions, and trypsin as the digestion enzyme. A maximum number of one missed cleavage was allowed, and carbamidomethylated cysteine and oxidized methionine were set as fixed and optional modifications, respectively. Only peptides with Mascot scores >30 were accepted. Scaffold (version 01_05_06, Proteome Software Inc., Portland, OR) was used to validate MS/MS-based peptide and protein identifications. Peptide identifications were accepted if they could be established at greater than 90.0% probability as specified by the Peptide Prophet algorithm (18). Protein identifications were accepted if they could be established at greater than 95.0% probability and contained at least two identified peptides. Protein probabilities were assigned by the Protein Prophet algorithm (19). Before we annotated a certain peptide derived from the xenograft-bearing mice as human, a stringent selection procedure was followed (see Fig. 1). First all peptide mass values identified in the serum from control mice and PC339 or PC346 xenograft-bearing mice were searched against both the International Protein Index (IPI) mouse and IPI human databases (version 3.18, containing 53,788 and 60,090 proteins, respectively). Then a selection was made of peptides uniquely present in the serum of PC346 or PC339 xenograft-bearing mice. These peptides were subsequently divided into a group of human-specific peptides (identified only in the IPI human database) and a group of homologous peptides (present in both the IPI human and IPI mouse databases). Homologous peptides were annotated as tumor-derived if four or more times higher abundant in the serum of PC339 or PC346 xenografted mice in comparison with control serum as listed in Scaffold. Additionally to double check human specificity, the identified human-specific peptides were blasted against the Swiss-Prot database of the National Center for Biotechnology Information (NCBI) database.

Two-dimensional SDS-PAGE Analysis of Proteasomes—To clean up samples from contaminants, for each xenograft-derived serum sample (50 μg of protein) the 2-D Clean-Up kit (Amersham Biosciences) was utilized according to the manufacturer's instructions. Next samples were solubilized in 125 μl of rehydration buffer (8 M urea, 2% CHAPS, 0.5% IPG buffer, 0.2% DTT, trace of bromphenol blue, all dissolved in H_2O). The samples were loaded onto Immobiline dry strip gels (pH 3–10, non-linear, 7 cm; Amersham Biosciences). Isoelectric focusing was carried out as follows: 30 V for 10 h, 300 V for 2 h, 1000 V for 30 min, 5000 V for 90 min, 5000 V for 30 min, and 20 V for 20 h. Before starting the second dimension, strips were reduced and alkylated for 15 min in DTT equilibration buffer (6 M urea, 50 mM Tris, pH 8.8, 20% glycerol, 2% SDS, 1% DTT) and iodoacetamide equilibration buffer (6 M urea, 50 mM Tris, pH 8.8, 20% glycerol, 2% SDS, 2.5% iodoacetamide). Next the IPG strips were placed upon a Criterion XT bis-Tris gel (12%; Bio-Rad). The second dimension was run at 100 V for ± 2 h with XT MOPS buffer (Bio-Rad). After running the second dimension, gels were blotted onto Protran nitrocellulose membrane in Tris-glycine-SDS buffer (Bio-Rad). The immunoblot was

blocked for 1 h and after washing twice incubated overnight at 4 °C with a monoclonal antibody (1:2000) against proteasome α subunits 6, 2, 4, 5, 1, and 3 (clone MCP231, Biomol International, Exeter, UK). This corresponds with the α subunits 1, 2, 3, 5, 6, and 7 according to the nomenclature of Baumeister *et al.* (20). In addition, monoclonal antibodies specifically directed against the proteasome α1 subunit (PSMA1; α6 according to the Baumeister *et al.* (20) nomenclature) (clone MCP20, Biomol International) or α3 subunits (PSMA3; α7 according to the Baumeister *et al.* (20) nomenclature) (clone MCP72, Biomol International) were utilized. The immunoblot was washed and incubated for 1 h with a 1:1000 solution of a goat anti-mouse horse-radish peroxidase-conjugated antibody (DakoCytomation, Glostrup, Denmark). The secondary antibody was visualized with a chemilumi-nescence detection kit (Roche Applied Science). For reprobing, blots were immersed in a 0.04 M Tris-HCl, 0.06 M Tris base, 0.07 M SDS, 0.10 M β-mercaptoethanol solution for 20 min at 50 °C.

Native Gel Electrophoresis of Proteasomes—The protocol for characterization of the proteasome by native gel electrophoresis was followed as previously described by Elsasser *et al.* (21). Depleted xenograft and control serum samples were mixed with 5× sample buffer containing 250 mM Tris-HCl, pH 7.4, 50% glycerol, 60 ng/ml xylene cyanol. Samples were either directly loaded or denatured by heating at 96 °C for 5 min. Gels were run for 3–4 h at 4 °C. Gels were transferred onto Protran nitrocellulose membranes at 250 mA for 1.5 h.

Sandwich ELISA for Quantification of the Proteasome—Serum proteasome concentrations were measured as previously described by Dutaud *et al.* (22) with some minor modifications. Briefly serum from control ($n = 3$) and PC339 ($n = 3$) or PC346 ($n = 3$) xenograft-bearing mice (1:20 diluted) was incubated for 1 h on a plate coated with a 1:4500 dilution of a monoclonal antibody against PSMA1 (clone MCP20, Biomol International). After addition of a 1:1500 solution of a rabbit anti-proteasome antibody (directed against β subunits of the proteasome; PW 8155, Biomol International) cells were extensively washed with PBS-Tween 20 buffer. Then a 1:4000 solution of goat anti-rabbit horseradish peroxidase-conjugated antibody (Dako-Cytomation) was added, and the plate was incubated for 1 h in the dark. To reveal horseradish peroxidase activity, 50 mM phosphate, 25 mM citrate buffer, pH 5.0 was added to the cells. After 15 min, the reaction was stopped with 2.5 M sulfuric acid. Absorbance values were measured at 492 nm. All analyses were performed in triplicate.

Cell Culture and Isolation of PC346C and VCaP-derived Exosomes—The human prostate cancer cell line PC346C was cultured in Dulbecco's modified Eagle's medium-Ham's F-12 medium (Cambrex Bio Science, Verviers, Belgium) supplemented with 0.1 nM R1881, 2% FCS (PAN Biotech, Aidenbach, Germany), 1% insulin-transferrin-selenium (Invitrogen), 0.01% BSA (Roche Applied Science), 10 ng/ml epidermal growth factor (Sigma-Aldrich), 100 units/ml penicillin and 100 μg/ml streptomycin antibiotics (Cambrex Bio Science), 100 ng/ml fibronectin (Harbor Bio-Products, Tebu-bio, the Netherlands), 20 μg/ml fetuin (ICN Biomedicals, Zoetermeer, The Netherlands), 50 ng/ml cholera toxin (Sigma-Aldrich), 0.1 mM phosphoethanolamine (Sigma-Aldrich), and 0.6 ng/ml triiodothyronine (Sigma-Aldrich) (23). The human PCa cell line VCaP was cultured in RPMI 1640 medium (Cambrex Bio Science) supplemented with 10% dextran-coated charcoal-treated FCS (PAN Biotech) and 100 units/ml penicillin and 100 μg/ml streptomycin antibiotics (Cambrex Bio Science). Exo-somes were isolated according to the protocol described previously by Hegmans *et al.* (24). Briefly PC346C and VCaP were cultured in their respective medium to 80% confluency. Cultures were washed twice with PBS and incubated for 48 h in a humidified atmosphere of 5% CO_2, 95% air with serum-free medium consisting of Dulbecco's modified Eagle's medium-Ham's F-12 or RPMI 1640 medium (Cambrex Bio Science) supplemented with 0.1 nM R1881. After incubation

cell culture supernatants were subjected to successive centrifuga-tions of $400 \times g$ (10 min), $3000 \times g$ (20 min), and $10,000 \times g$ (30 min). Exosomes were then pelleted at $64,000 \times g$ for 110 min using an SW28 rotor (Beckman Coulter Instruments, Fullerton, CA). Exosome pellets were resuspended in 0.32 M sucrose and centrifuged at $100,000 \times g$ for 1 h (SW60 rotor, Beckman Coulter Instruments).

For several experiments, the isolated exosomes from PC346C were further purified by immobilization onto magnetic beads. In short, 25 μl of Dynabeads, precoated with goat anti-mouse immune globulin G (Invitrogen Dynal AS, Oslo, Norway) were incubated for 1 h with 30 μl of an anti-CD9 monoclonal antibody (clone MM2/57, Chemicon International, London, UK). Thereafter beads were incubated by ro-tation top end over with 20 μg of exosomes for 1 h at 4 °C. After washing four times, beads and exosomes were resuspended in PBS for further experiments.

Electron Microscopy of Isolated Exosomes—Exosomes from PC346C obtained after ultracentrifugation of cell culture supernatants were resuspended in 10 μl of Milli-Q and spotted onto Formvar-coated grids (200 mesh). Adsorbed exosomes were fixed in 2% paraformaldehyde for 5 min at room temperature. After fixation the exosomes were either directly negatively stained using uranyl acetate or immunolabeled with antibodies against CD9 (clone MM2/57, Chemicon International). Antigen-antibody complexes were visual-ized with protein A conjugated with 10-nm colloidal gold particles (1:20 dilution; Aurion, Wageningen, The Netherlands) followed by negative staining (see above). The specificity of the labeling proce-dure was tested by omitting the primary antibody. Grids were exam-ined by a Philips CM100 electron microscope at 80 kV.

Mass Spectrometry of Exosomes—After resuspending the exo-some pellet in PBS, 10 μg of isolated exosomes and 10 μg of supernatant fraction were applied onto two 10% SDS-polyacrylamide gels. After running, one of the gels was silver-stained as described previously by Mortz *et al.* (25). This gel was used to identify distinct bands present in the exosome fraction (see Fig. 4*b*). Subsequently these bands were excised from a Coomassie Brilliant Blue (Merck)-stained gel and cut in 3-mm sections. Preparation for mass spec-trometry was performed using the protocol described under "Prepa-ration of Xenograft Sera for Mass Spectrometry". Peptide separation was performed on a nanoscale liquid chromatography system (nanoLC Ultimate 3000) (Dionex, Sunnyvale, CA) with a 50-min gra-dient (5–40% acetonitrile, H_2O, 0.1% formic acid). The injection vol-ume was 5 μl of the tryptically digested sample. Peptides were separated on a C_{18} PepMap column (150 mm × 75 μm inner diam-eter) (Dionex) at 200 nl/min after preconcentration on a trap column (1 mm × 300 μm inner diameter). Separated peptides were detected by a linear ion trap Orbitrap (LTQ-Orbitrap) mass spectrometer (Finnigan LTQ Orbitrap XL, Thermo Electron). Samples were measured in a data-dependent acquisition mode. In the measurement method used, the peptide masses are measured in a survey scan at a maximum resolution of 60,000. To obtain a maximum mass accuracy a prescan is used to keep the ion population in the Orbitrap for each scan approximately the same. During the high resolution scan in the Orbi-trap the five most intense monoisotopic peaks in the spectra were fragmented and measured in the LTQ. The fragment ion masses were measured in the LTQ to have a maximum sensitivity and a maximum amount of MS/MS data.

For a full analysis of the exosomal proteome, 10 μg of the isolated exosome fraction was applied onto a 10% SDS-polyacrylamide gel and run for ~1.5 cm inside the running gel. Thereafter this gel section was excised and divided into 3-mm sections, washed, destained (100% acetonitrile followed by 50 mM ammonium bicarbonate), de-hydrated (100% acetonitrile), and reduced with 6.5 mM DTT in 50 mM ammonium bicarbonate for 45 min at 60 °C. After alkylation with 54 mM iodoacetamide in 50 mM ammonium bicarbonate, proteins were

dehydrated in 100% acetonitrile and then rehydrated with the digestion solution containing 10 ng/μl ultra grade sequencing trypsin (Promega) for 30 min on ice. After removal of the redundant trypsin solution and addition of 50 mM ammonium bicarbonate solution to cover the gel pieces, gel particles were incubated overnight at 37 °C. After extraction, the peptides were dissolved in 5% formic acid and stored at −80 °C until analysis. Mass spectrometry was performed using the protocol described under "Liquid Chromatography-Mass Spectrometry of Xenograft Sera." For protein identification, database searches were performed using Mascot version 2.2 (Matrix Science) allowing 5-ppm mass deviation for the precursor ion, a 0.6-Da tolerance on the fragment ions, and trypsin as the digestion enzyme. A maximum number of one missed cleavage was allowed, and carbamidomethylated cysteine and oxidized methionine were set as fixed and optional modifications, respectively. All peptide mass values identified in the isolated exosomes were searched against the IPI human database (version 3.37, containing 69,164 proteins). Only peptides with Mascot scores >30 were accepted. Scaffold (version 2_01_02, Proteome Software Inc., Portland, OR) was used to validate MS/MS-based peptide and protein identifications. Peptide identifications were accepted if they could be established at greater than 90.0% probability as specified by the Peptide Prophet algorithm (18). Protein identifications were accepted if they could be established at greater than 95.0% probability and contained at least two identified peptides. Protein probabilities were assigned by the Protein Prophet algorithm (19).

One-dimensional SDS-PAGE Analysis and Western Blotting—For one-dimensional electrophoresis, samples containing 10 μg of protein were mixed with Laemmli sample buffer (1:1 ratio) and loaded onto 10% SDS-polyacrylamide gels. Gels were transferred onto a Protran nitrocellulose membrane for Western blotting. The following antibodies were used: CD9 (1:500 dilution; clone MM2/57, Chemicon International), RAB5A (1:200 dilution; clone FL-215, Santa Cruz Biotechnology, Santa Cruz, CA), RAB11A (1:100 dilution; Invitrogen), hepatocyte growth factor-regulated tyrosine kinase substrate (HGS; previously known as HRS; 1:500 dilution; Alexis Biochemicals, San Diego, CA), GAPDH (1:500 dilution; clone 7B, LabFrontier, Seoul, Korea), ENO1 (1:1000 dilution; clone H300, Santa Cruz Biotechnology), 14-3-3θ (1:1000 dilution; clone 3B9, Calbiochem, San Diego, CA), PSA (1:500 dilution; clone A0562, DakoCytomation), proteasome α subunits 6, 2, 4, 5, 1, and 3 (1:2000 dilution; clone MCP231, Biomol International), PSMA1 (1:1000 dilution; clone MCP20, Biomol International), PSMA3 (1:1000 dilution; clone MCP72, Biomol International), and proteasome subunit β1 (PSMB1; β6 according to the Baumeister *et al.* (20) nomenclature; Biomol International).

Isolation and Analysis of Exosomal RNA—Exosomal total RNA was isolated using the RNeasy Mini kit (Qiagen, Hilden, Germany) as described by Valadi *et al.* (16). In short, pelleted exosomes were disrupted and homogenized in 350 μl of buffer RLT (Qiagen), and 1050 μl of 100% ethanol was added before samples were transferred to the RNeasy Mini spin column. Hereafter the procedure was followed as described by the manufacturer's protocol.

Analysis of RNA expression was performed by RT-PCR. One microgram of exosomal RNA was reverse transcribed using Moloney murine leukemia virus reverse transcriptase (Invitrogen) and an oligo-(dT)$_{12}$ primer. Primer combinations used were as follows: PSA-4A (5′-ACGTGTGTGCAAGTTCACC-3′) and PSA-5B (5′-TGTACAGG-GAAGGCCTTTCG-3′), TMPRSS2-E1 (5′-AGCGCGGCAGGAAGC-CTTA-3′) and ERG-R (5′-GTAGGCACACTCAAACAACGACTGG-3′), and GAPDH 462U17 (5′-CATGTTCGTCATGGGTG-3′) and GAPDH 589L20 (5′-ACTGTGGTCATGAGTCCTTC-3′). PCR was performed for 27 cycles at an annealing temperature of 58 °C.
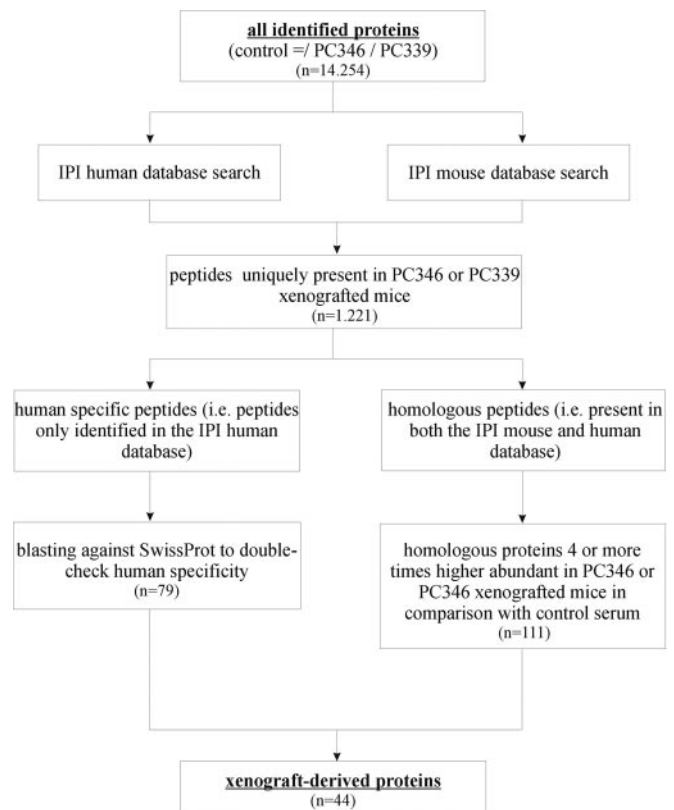

FIG. 1. **The selection procedure followed to annotate identified proteins as tumor-derived proteins.**

RESULTS

Identification of 44 Tumor-derived Proteins in Xenografted Mice—The selection procedure followed to annotate identified proteins as tumor-derived in the circulation of human prostate cancer-xenografted mice is depicted in Fig. 1. After serum collection from control mice (n = 9) and PC346 (n = 9) and PC339 (n = 9) xenografted mice, samples were pooled and depleted of high abundance proteins, and proteins were separated by one-dimensional gel electrophoresis. Following tryptic digestion, peptides were subsequently analyzed by LTQ-FT-ICR-MS/MS. After data analysis (supplemental materials and methods), 44 proteins were identified as tumor-derived (at greater than 95.0% probability and with two or more identified peptides) (Table I). Of those, 22 were annotated as cytoplasmic proteins by the Gene Ontology database. The cytoplasmic proteins contained 12 of the subunits of the proteasome of which seven were identified based on the presence of human-specific peptides in the serum of xenograft-bearing mice.

Validation and Characterization of Proteasome Subunits in Xenograft Sera—To specify and validate the presence of tumor-derived proteasome subunits in the circulation of the xenografted mice, two-dimensional SDS-PAGE analysis of xenograft-derived serum samples was performed. Fig. 2 shows a comparison between serum from control mice (n = 3)

TABLE I

List of 44 proteins annotated as tumor-derived proteins in xenograft-bearing mice

Identified peptides were divided into a group of human specific peptides (identified only in the IPI human database) and a group of homologous peptides (present in both the IPI human and IPI mouse database). Homologous peptides were annotated as tumor-derived when 4 or more times higher abundant in the serum of PC339 or PC346 xenografted-mice in comparison with control serum. Annotations are derived from the Gene Ontology database.

Protein name	Gene symbol	IPI accession no.	Human/homologue	No. of unique peptides	Sequence coverage (%)	Xenograft	Molecular function	Biological process	Location
14-3-3 protein γ[a]	YWHAG	IPI00230707	Homologue	5	20.65	PC339	Protein kinase C binding	Regulation of signal transduction	Cytoplasm
14-3-3 protein θ[a]	YWHAQ	IPI00018146	Human	4	15.92	PC339	Protein kinase C inhibitor activity	Regulation of progression through cell cycle	Cytoplasm
α-Enolase[a]	ENO1	IPI00465248	Human	4	26.67	PC339	Phosphopyruvate hydratase activity	Glycolysis	Cytoplasm
Apolipoprotein A-I precursor	APOA1	IPI00021841	Human	3	16.24	PC339	Lipid binding	Cholesterol metabolism	Secreted
Cathepsin Z precursor	CTSZ	IPI00002745	Homologue	2	5.61	PC346	Cysteine-type peptidase activity	Proteolysis	Lysosome
Chromosome 20 orf 114	C20orf114	IPI00291410	Human	2	4.34	PC346	Lipid binding		
Coactosin-like protein	COTL1	IPI00017704	Homologue	2	9.15	PC339	Actin binding		
Coagulation factor V	F5	IPI00406603	Homologue	6	3.55	PC339	Oxidoreductase activity	Blood coagulation	Secreted
Cofilin, non-muscle isoform[a]	CFL1	IPI00012011	Homologue	3	21.69	PC339	Protein binding	Cytoskeleton organization and biogenesis	Cytoplasm
Complement component C8 β chain precursor	C8B	IPI00294395	Homologue	2	5.66	PC339		Immune response	Secreted
Cytochrome c	CYCS	IPI00465315	Homologue	2	17.14	PC346/339	Heme binding	Caspase activation via cytochrome c	Mitochondrion matrix
Fructose-bisphosphate aldolase A[a]	ALDOA	IPI00465439	Human/homologue	11	30.77	PC346/339	Fructose-bisphosphate aldolase activity	Glycolysis	
Glutathione peroxidase 3 precursor	GPX3	IPI00026199	Human	5	23.01	PC339	Glutathione peroxidase activity	Hydrogen peroxide catabolism	Secreted
Glyceraldehyde-3-phosphate dehydrogenase[a]	GAPDH	IPI00219018	Human	7	25.97	PC346/339	Glyceraldehyde-3-phosphate dehydrogenase activity		Cytoplasm
Inter-α (globulin) inhibitor H3[a]	ITIH3	IPI00028413	Homologue	2	3.03	PC346	Serine-type endopeptidase inhibitor activity	Hyaluronan metabolism	Secreted
Junction plakoglobin	JUP	IPI00554711	Homologue	2	2.81	PC339	Cytoskeletal protein binding	Cell adhesion	
Lactate dehydrogenase A[a]	LDHA	IPI00217966	Human/homologue	9	21.69	PC346/339	L-Lactate dehydrogenase activity	Anaerobic glycolysis	Cytoplasm
Lactate dehydrogenase B[a]	LDHB	IPI00219217	Human	10	29.94	PC346/339	L-Lactate dehydrogenase activity	Anaerobic glycolysis	Cytoplasm
Lumican precursor	LUM	IPI00020986	Homologue	2	5.92	PC339	Collagen binding	Collagen fibril organization	Secreted
Lysozyme C precursor	LYZ	IPI00019038	Human/homologue	4	23.65	PC346/339	Lysozyme activity	Inflammatory response	
Maltase-glucoamylase, intestinal[a]	MGAM	IPI00220143	Human	3	1.18	PC346/339	Protein binding	Carbohydrate metabolism	Cell membrane
Myosin heavy chain, skeletal muscle, adult 2	MYH2	IPI00007856	Homologue	3	4.94	PC346	Actin binding		
Myosin, light polypeptide 6, alkali, smooth muscle and non-muscle isoform 1	MYL6B	IPI00335168 IPI00413922	Homologue	3	14.42	PC339	Structural component of muscle	Muscle filament sliding	
Nucleoside-diphosphate kinase A	NME1	IPI00012048	Human/homologue	6	46.71	PC339	Nucleoside-diphosphate kinase activity	Negative regulation of cell proliferation	Cytoplasm
Nucleoside-diphosphate kinase B	NME2	IPI00026260	Homologue	6	42.76	PC339	Nucleoside-diphosphate kinase activity	Negative regulation of cell proliferation	Cytoplasm

TABLE I—*continued*

Protein name	Gene symbol	IPI accession no.	Human/homologue	No. of unique peptides	Sequence coverage	Xenograft	Molecular function	Biological process	Location
					%				
Peroxiredoxin-2[a]	PRDX2	IPI00000874 IPI00027350	Human/homologue	3	13.13	PC339	Thioredoxin peroxidase activity	Antiapoptosis	Cytoplasm
Proteasome subunit α type 1	PSMA1	IPI00472442	Human/homologue	6	24.91	PC346/339	Peptidase activity	Proteolysis	Cytoplasm
Proteasome subunit α type 2	PSMA2	IPI00219622	Homologue	5	22.64	PC346/339	Peptidase activity	Proteolysis	Cytoplasm
Proteasome subunit α type 4	PSMA4	IPI00299155	Human	5	17.30	PC339	Peptidase activity	Proteolysis	Cytoplasm
Proteasome subunit α type 6	PSMA6	IPI00029623	Homologue	9	37.80	PC346	Peptidase activity	Proteolysis	Cytoplasm
Proteasome subunit α type 7	PSMA7	IPI00024175	Human	6	21.37	PC339	Peptidase activity	Proteolysis	Cytoplasm
Proteasome subunit β type 1	PSMB1	IPI00025019	Human/homologue	7	34.02	PC346/339	Peptidase activity	Proteolysis	Cytoplasm
Proteasome subunit β type 2	PSMB2	IPI00028006	Homologue	2	12.44	PC346	Peptidase activity	Proteolysis	Cytoplasm
Proteasome subunit β type 3[a]	PSMB3	IPI00028004	Homologue	3	18.05	PC346/339	Peptidase activity	Proteolysis	Cytoplasm
Proteasome subunit β type 4	PSMB4	IPI00556607	Human/homologue	5	17.80	PC346/339	Peptidase activity	Proteolysis	Cytoplasm
Proteasome subunit β type 5	PSMB5	IPI00479306	Human/homologue	10	38.78	PC346/339	Peptidase activity	Proteolysis	Cytoplasm
Proteasome subunit β type 6	PSMB6	IPI00000811	Human	3	12.97	PC346/339	Peptidase activity	Proteolysis	Cytoplasm
Proteasome subunit β type 8	PSMB8	IPI00000783	Homologue	2	5.88	PC346	Protein binding	Proteolysis	Cytoplasm
Prothrombin precursor	F2	IPI00019568	Homologue	2	2.25	PC346	Thrombin activity	Regulation of progression through cell cycle	Secreted
Splice isoform 1 of complement factor B precursor	CFP	IPI00639937	Homologue	2	4.90	PC346/339	Complement binding	Complement activation	Secreted
Thrombospondin-1 precursor[a]	THBS1	IPI00296099	Homologue	7	7.26	PC346/339	Signal transducer activity	Cell motility	Secreted
Transcobalamin-2	TCN2	IPI00136556	Homologue	3	6.09	PC339	Cobalamin transporter activity	Cobalamin transport	Secreted
Triose-phosphate isomerase 1 variant[a]	TPI1	IPI00465028	Human/homologue	5	22.09	PC346/339	Triose-phosphate isomerase activity	Glycolysis	
Voltage-dependent anion channel 2	VDAC2	IPI00455531	Homologue	2	7.77	PC346	Voltage-gated anion channel porin activity	Anion transport	Mitochondrion outer membrane

[a] Proteins that have earlier been identified by others in isolated exosomes from various origin.

and serum from PC339 ($n = 3$) and PC346 ($n = 3$) xenografted mice. Proteasome subunits were detected using a monoclonal antibody directed against α subunits 6, 2, 4, 5, 1, and 3 of the proteasome. Strong signals were observed in the
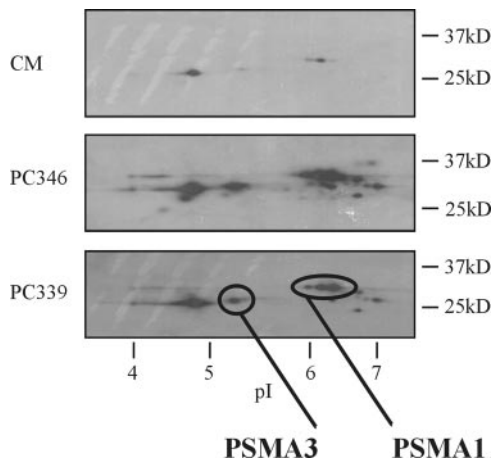

FIG. 2. **2D PAGE Western blotting analysis of depleted serum from control mice (*CM*), PC346 xenograft-bearing mice (PC346), and PC339 xenograft-bearing mice (PC339).** Spots were detected by using a monoclonal antibody to proteasome α subunits 6, 2, 4, 5, 1, and 3. The presence of PSMA1 and PSMA3 proteasome subunits was confirmed with specific monoclonal antibodies. Strong signals are visible in the serum from both the PC346 and PC339 mice. Also faint signals were detected in the control serum because of cross-reactivity with mouse proteasome subunits, which are present under normal conditions in the mouse serum.

serum from both the PC346 and PC339 xenografted mice. As the proteasome antibody recognizes both mouse and human proteasome subunits, also faint signals were visible in the control serum that are known to be normally present in the mouse circulation. This is in line with the identification of mouse-specific proteasome peptides as detected by FT-ICR-MS/MS (data not shown). After stripping, blots were reprobed, and two of the spots could be specifically identified in the serum of PC339 and PC346 xenografted mice as the PSMA1 and PSMA3 subunits by using specific monoclonal antibodies directed against these proteins. The identified spots were consistent regarding molecular weight and pI with an earlier study performed by Claverol *et al.* (26).

Proteasome Subunits Are Circulating as a Complex in Xenograft Sera—To investigate whether the identified proteasome subunits were present as proteasome complexes in the serum of xenografted mice, native gel electrophoresis of control serum and serum from xenograft-bearing mice was performed. Fig. 3*a* shows the presence of high molecular weight proteasome complexes in the xenograft sera. In both the 12.5% gel and 3.5% gel high molecular weight complexes are visible in the samples that were run under native conditions. After denaturation, the high molecular weight complexes disappeared, indicating disintegration into single proteasome subunits. The same effect is seen in the endogenous proteasome subunits of the control mouse.

The presence of intact proteasome complexes was also investigated by sandwich ELISA. Serum samples from control

FIG. 3. *a*, native 1D gel electrophoresis of serum from control mice (*CM*) and PC346 or PC339 xenograft-bearing mice showing the presence of intact proteasome complexes. High molecular weight complexes are visible under native conditions in both 12.5 and 3.5% gels. After denaturation, mostly single subunits are visible in the 12.5% gel, and the high molecular weight complexes in the 3.5% gel have disappeared. Bands were detected by a monoclonal antibody directed against the PSMA1 subunit of the proteasome. *b*, proteasome concentrations in xenograft-bearing mice and control mice serum samples under native (*left*) and denatured (*right*) conditions as measured by sandwich ELISA. After serum denaturation proteasome levels are strongly diminished, indicating the existence of proteasome complexes in xenograft and control serum samples. *Error bars* represent standard deviations.
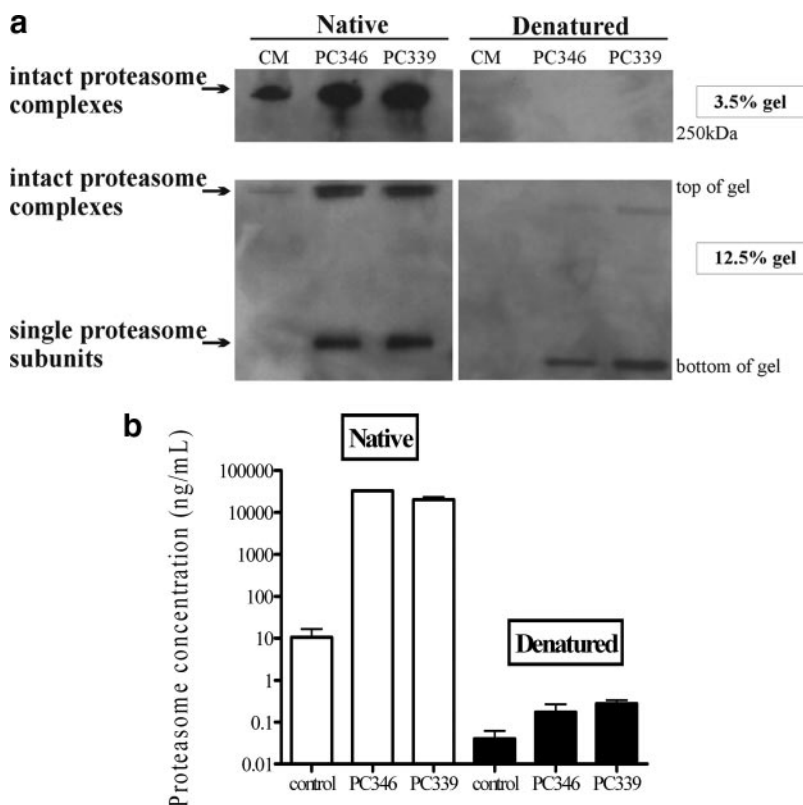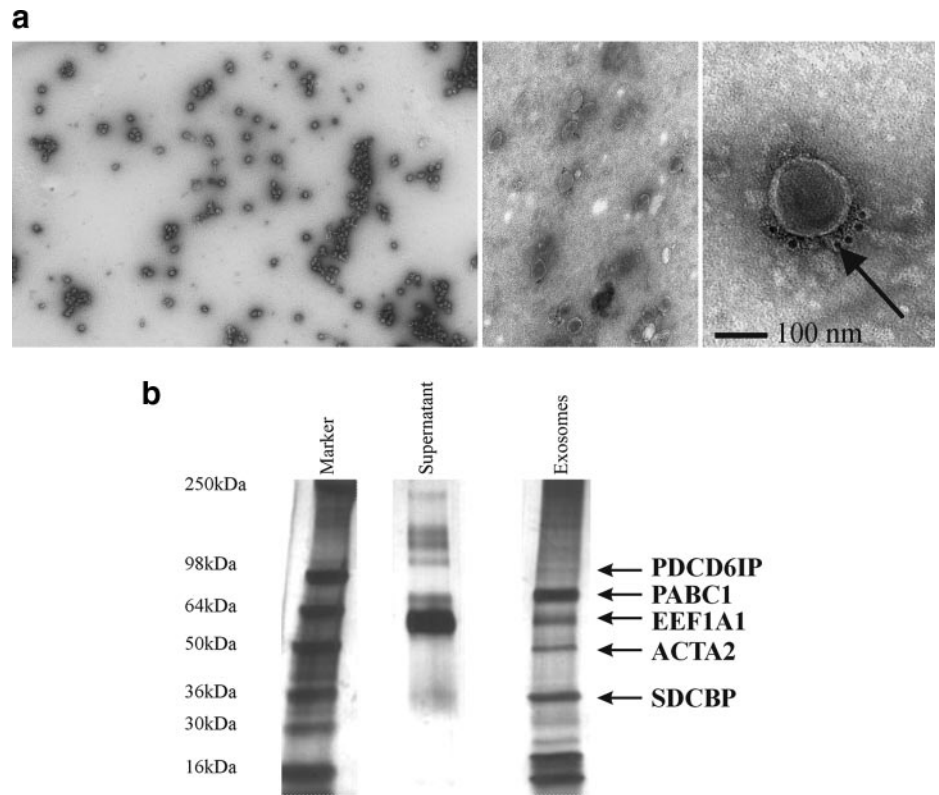
FIG. 4. *a*, electron microscopy of exosomes isolated from the PC346C cell line. *Left*, electron micrograph of negatively stained exosomes showing a homogenous mixture of isolated vesicles; *middle*, ImmunoGold labeling of exosomes with the exosomal marker CD9 (Tetraspanin 29); *right*, increased magnification of the *middle* image shows positive CD9 membrane staining of exosomes (see *arrow*). *b*, separation of PC346C cell-derived exosomal proteins by 1D SDS-PAGE followed by silver staining. The indicated protein bands were excised and identified by LTQ-Orbitrap. *SDCBP*, syndecan-binding protein.

($n = 3$) and xenograft mice ($n = 6$) were diluted 1:20 and analyzed in triplicate under native conditions and after denaturation by heating at 96 °C for 5 min. Proteasome levels (mean ± S.D.) under native conditions in control, PC346, and PC339 serum were 10.5 ± 10.6, 32,759 ± 1720.0, and 20,339 ± 5062.2 ng/ml, respectively. After denaturation, proteasome concentrations (mean ± S.D.) decreased to 0.040 ± 0.03, 0.17 ± 0.16, and 0.28 ± 0.10 ng/ml in control, PC346, and PC339 serum, respectively (Fig. 3*b*). Because the capture antibody of the sandwich ELISA is directed against the α1 subunit (PSMA1) of the proteasome whereas the detection antibody is directed against β subunits, this confirms the presence of proteasome complexes in the serum of the xenografted mice.

Electron Microscopy of Isolated Exosomes—A large portion of the cytoplasmic tumor-derived proteins identified in the xenograft model has previously been identified as part of the human exosomal protein content. To explore the origin of the cytoplasmic proteins identified in the xenograft serum, exosomes were isolated from the PC346C cell line. To confirm that the structures isolated were indeed exosomes, they were examined by electron microscopy (Fig. 4*a*). This showed a homogenous mixture of small bilayer membrane vesicles with an average diameter of 140 nm. ImmunoGold labeling of exosomes with an antibody to CD9 (Tetraspanin 29), an established marker for tumor cell-derived exosomes, showed positive exosome membrane staining (Fig. 4*a*).

Proteomics Analysis of Exosomes—Supernatant and exosome fractions of the PC346C cell line were separated by 1D SDS-PAGE followed by silver staining (Fig. 4*b*). The exosome fractions showed several distinct bands, which were absent in the supernatant fraction. Several bands were excised and subjected to LTQ-Orbitrap mass spectrometry (MS/MS) leading to the identification of five proteins: programmed cell death 6 protein (PDCD6IP; 10 unique peptides, 10.65% sequence coverage), poly(A)-binding protein 1 (PABC1; 12 unique peptides, 18.71% sequence coverage), eukaryotic translation elongation factor 1 α1 (EEF1A1; three unique peptides, 6.28% sequence coverage), α-actin-2 (ACTA2; 13 unique peptides, 45.62% sequence coverage), and syndecan-binding protein (syntenin; four unique peptides, 14.77% sequence coverage).

An in-depth proteomics analysis of the whole exosome fraction was performed by LTQ-FT-ICR-MS/MS. A total of 48 unique proteins were discovered in the exosome fraction of the PC346C cell line at a protein identification probability of ≥99% and ≥2 peptides per protein (Table II). At a protein probability of ≥99% and ≥1 peptide per protein 126 proteins were identified. Among those proteins identified with two or more peptides per protein were two of the proteins that had earlier been identified in the serum of xenograft-bearing mice (GAPDH and lactate dehydrogenase B) (12). Also the presence of the exosomal marker CD9 and the prostate-specific protein folate hydrolase 1 (FOLH1; prostate-specific membrane antigen) were confirmed. ENO1 and fructose-bisphos-

TABLE II

List of 48 proteins identified by two or more peptides in the exosome fraction of the PC346C cell line

Annotations are derived from the Gene Ontology database.

Protein name	Gene symbol	Protein accession no.	No. of unique peptides	Sequence coverage (%)	Molecular function	Biological process	Location
Actin, γ 1	ACTG1	IPI00021440	15	40.30	Structural constituent of cytoskeleton	Cell motility	Cytoplasm
ADAM metallopeptidase domain 10	ADAM10	IPI00013897	3	3.88	Protein homodimerization activity	Protein amino acid phosphorylation	Cell membrane
ADAM metallopeptidase domain 15	ADAM15	IPI00013302	4	6.39	Proteolysis and peptidolysis	Cell adhesion	Cell membrane
Annexin A2	ANXA2	IPI00418169	7	24.90	Phospholipase inhibitor activity	Skeletal development	Secreted protein
Annexin A6	ANXA6	IPI00002459	3	7.20	Calcium ion binding		Cell membrane
ATPase, Na$^+$/K$^+$-transporting, α 1 polypeptide	ATP1A1	IPI00006482	5	5.96	Sodium;potassium-exchanging ATPase activity	Sodium ion transport	Cell membrane
Brain-abundant, membrane-attached signal protein 1	BASP1	IPI00299024	4	40.10			Cell membrane
Chromosome 1 open reading frame 58	C1orf58	IPI00065500	2	10.70			
Capping protein (actin filament) muscle Z-line, α 1	CAPZA1	IPI00005969	2	7.69	Actin binding	Cell motility	
CD151 molecule (Tetraspanin 24)	CD151	IPI00298851	2	5.93	Protein binding	Cell adhesion	Cell membrane
CD2-associated protein	CD2AP	IPI00412771	6	11.60	Structural constituent of cytoskeleton	Cell migration	Cytoplasm
CD9 molecule	CD9	IPI00215997	3	15.40	Protein binding	Cell motility	Cell membrane
Chromatin-modifying protein 4B	CHMP4B	IPI00025974	2	8.93			Cytoplasm
Clathrin, heavy chain 1	CLTC	IPI00024067	10	6.81	Signal transducer activity	Receptor-mediated endocytosis	Cell membrane
Eukaryotic translation elongation factor 1 α 1	EEF1A1	IPI00396485	14	37.20	Translation elongation factor activity	Translation elongation	Cytoplasm
EH domain-containing protein 1	EHD1	IPI00017184	2	5.06	ATP binding		Cell membrane
F11 receptor	F11R	IPI00001754	5	16.40		Cell motility	Cell membrane
Family with sequence similarity 125, member A	FAM125A	IPI00744702	3	16.10			Cytoplasm
Formin-binding protein 1-like	FNBP1L	IPI00015580	2	3.47			Cytoplasm
Folate hydrolase (prostate-specific membrane antigen) 1	FOLH1	IPI00028514	7	12.30	Dipeptidase activity	Proteolysis	Cell membrane
Glyceraldehyde-3-phosphate dehydrogenase	GAPDH	IPI00219018	3	14.00	Glyceraldehyde-3-phosphate dehydrogenase activity	Glycolysis	Cytoplasm
Histone cluster 1, H1c	HIST1H1C	IPI00217465	2	10.30	DNA binding	Nucleosome assembly	Nucleus
Histone cluster 1, H2ab	HIST1H2AB	IPI00026272	2	21.50	DNA binding	Nucleosome assembly	Nucleus
Heat shock protein 90 kDa α (cytosolic), class B member 1	HSP90AB1	IPI00334775	4	6.49	Unfolded protein binding	Response to unfolded protein	Cytoplasm
Heat shock 70-kDa protein 1B	HSPA1B	IPI00807640	6	16.50	Unfolded protein binding	Antiapoptosis	Cytoplasm
Heat shock 70-kDa protein 8	HSPA8	IPI00003865	13	25.50	ATPase activity	Protein folding	Cytoplasm
Immunoglobulin superfamily, member 8	IGSF8	IPI00056478	6	12.60	Protein binding	Cell motility	Cell membrane
Integrin β-1	ITGB1	IPI00217563	3	3.89	Protein heterodimerization activity	Cell migration	Cell membrane
Lactate dehydrogenase B	LDHB	IPI00219217	2	7.78	L-Lactate dehydrogenase activity	Anaerobic glycolysis	Cytoplasm
Milk fat globule-EGF factor 8 protein	MFGE8	IPI00002236	2	4.91		Cell adhesion	Cell membrane
Poly(A)-binding protein, cytoplasmic 1	PABPC1	IPI00008524	16	25.90	Translation activator activity	mRNA stabilization	Cytoplasm
Poly(A)-binding protein, cytoplasmic 4	PABPC4	IPI00555747	5	18.40	Protein/RNA binding	RNA processing	Cytoplasm
Protein kinase C and casein kinase substrate in neurons 2	PACSIN2	IPI00027009	4	8.85	Transporter activity	Intracellular protein transport	Cytoplasm
Poly(rC)-binding protein 2	PCBP2	IPI00012066	2	7.46	Protein/RNA binding	mRNA metabolic process	Cytoplasm
Programmed cell death 6-interacting protein	PDCD6IP	IPI00246058	21	22.40	Signal transducer activity	Apoptosis	Cytoplasm
Prostaglandin F$_2$ receptor negative regulator	PTGFRN	IPI00022048	7	9.33	Protein binding	Negative regulation of protein biosynthetic process	Cell membrane

TABLE II—continued

Protein name	Gene symbol	Protein accession no.	No. of unique peptides	Sequence coverage	Molecular function	Biological process	Location
				%			
Ribosomal protein S27a	RPS27A	IPI00179330	5	31.40	Structural constituent of ribosome	Translation	Cytoplasm
Syndecan-binding protein (syntenin)	SDCBP	IPI00299086	3	15.10	Protein heterodimerization activity	Cell migration	Cell membrane
Serine incorporator 5	SERINC5	IPI00328883	2	4.97			Cell membrane
SH3-domain GRB2-like 1	SH3GL1	IPI00019169	8	23.60	Protein binding	Signal transduction	Cell membrane
Solute carrier family 3, member 2	SLC3A2	IPI00027493	2	5.48	Catalytic activity	Amino acid transport	Cell membrane
Sphingomyelin phosphodiesterase, acid-like 3B	SMPDL3B	IPI00550115	2	4.73	Hydrolase activity	Carbohydrate metabolism	Secreted protein
Sorting nexin-9	SNX9	IPI00001883	2	5.38	Protein binding	Protein localization	
Tumor-associated calcium signal transducer 1	TACSTD1	IPI00296215	5	21.30			Cell membrane
Tumor susceptibility gene 101 protein	TSG101	IPI00018434	7	21.30	Transcription corepressor activity	Regulation of cell growth	Cytoplasm
Tubulin, β	TUBB	IPI00011654	3	7.43	Structural constituent of cytoskeleton	Spindle assembly	
Vacuolar protein sorting 37 homolog B	VPS37B	IPI00002926	3	10.20			
Tyrosine 3-monooxygenase/tryptophan 5-monooxygenase activation protein, ζ polypeptide	YWHAZ	IPI00021263	5	22.90	Transcription factor binding	Signal transduction	Cytoplasm

phate aldolase A, also previously identified in the serum of xenograft-bearing mice, were positively identified at a probability of one peptide per protein (data not shown). All proteins identified in the specific exosome bands but ACTA2 (Fig. 4*b*) were also recovered in the in-depth proteomics analysis.

Analysis of Exosomes by One-dimensional SDS-PAGE Analysis—One-dimensional SDS-PAGE and Western blotting were performed to verify the presence in exosomes of several proteins previously identified by LTQ-FT-ICR-MS/MS in the xenograft model. CD9, RAB5A, RAB11A, HRS, GAPDH, and 14-3-3 protein θ (YWHAQ) were uniquely present in the isolated exosome fraction and could not be detected in the PC346C cell line supernatant, whereas α-enolase (ENO1) and α subunits of the proteasome were present in both fractions. PSA was uniquely present in the supernatant fraction and could not be detected in the isolated exosomes (Fig. 5*a*).

To certify that the proteasome subunits present in the exosome fraction were not the result of simultaneous pelleting of exosomes and proteasome complexes during ultracentrifugation, exosomes were further purified by magnetic beads coated with a CD9 antibody. After exosomal purification, bead-exosome complexes were loaded onto one-dimensional SDS-polyacrylamide gels. Blots were incubated with a monoclonal antibody to CD9 (Chemicon International) or a polyclonal antibody against the PSMB1 subunit of the proteasome. Fig. 5*b* shows that both the CD9 and PSMB1 subunit signals are visible in the exosome fraction as well as in the immunobead-purified exosome fraction.

Analysis of Exosomal RNA—As the PCa-specific *TM-PRSS2-ERG* gene fusion is expressed in the majority of PCa patients, we analyzed exosomes for the presence of the gene fusion product (27, 28). RNA was isolated from PC346C and VCaP cells and analyzed by RT-PCR. Both cell lines express PSA, whereas the *TMPRSS2-ERG* gene fusion is only present in VCaP and not in PC346 cells (27). KLK3 (PSA) and GAPDH RNAs were present in both VCaP and PC346C exosomes as well as in the total RNA fraction from both cell lines. The gene fusion product *TMPRSS2-ERG* was only detected in VCaP exosomes and in the VCaP cell line and was not detected in PC346C-derived exosomes and the PC346C cell line (Fig. 6).

DISCUSSION

The present study shows the identification of 44 tumor-derived proteins by mass spectrometry in xenograft models for PCa. Virtually all subunits of the proteasome were among the proteins identified, a finding that was verified by two-dimensional gel electrophoresis of xenograft-bearing and control mouse sera. Several of these proteasome subunits are part of the normal human plasma proteome as was shown by the Human Proteome Organisation Plasma Proteome Project (13). Increased proteasome levels have been related to hematological malignancies, especially multiple myeloma (29), but also to solid tumors, such as melanoma and colon carcinoma (30). Recently Byrne *et al.* (31) identified the proteasome β6
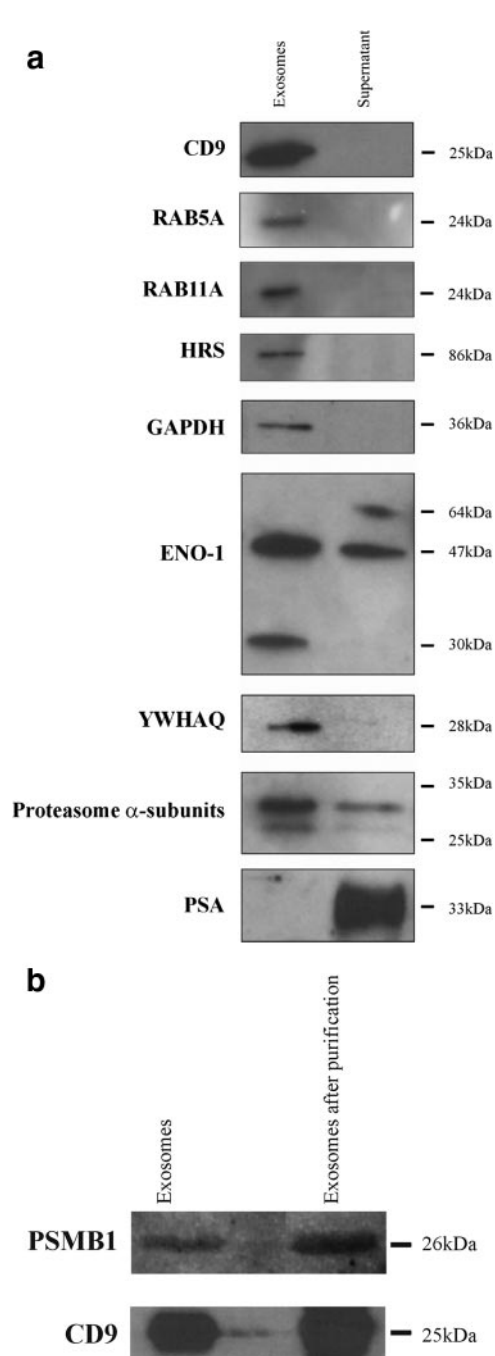
Fig. 5. *a*, 1D PAGE and Western blotting analysis comparing the exosome and supernatant fractions of the PC346C cell line for CD9, the members of the RAS oncogene family RAB5A and RAB11A, HRS, GAPDH, ENO1, YWHAQ (14-3-3 protein θ), proteasome α subunits, and PSA. CD9, RAB5A, RAB11A, HRS, GAPDH, and YWHAQ were uniquely identified in the isolated exosomes, whereas PSA could only be detected in the supernatant of the PC346C cell line. *b*, 1D PAGE and Western blotting analysis of the exosome fraction after purification with magnetic beads. This figure shows that the CD9 and proteasome β1 (PSMB1) signals are visible in the exosome fraction both before and after purification with magnetic beads, indicating that proteasome subunits are present inside exosomes or exosomal membranes.
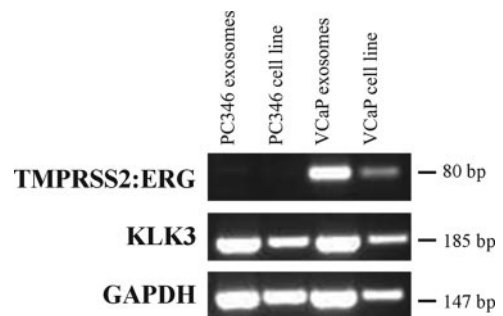
Fig. 6. **RT-PCR analysis of VCaP and PC346C cell lines and exosomes.** The *TMPRSS2-ERG* fusion gene is exclusively expressed in both the VCaP cell line and exosomes, whereas both cell lines and exosomes express KLK3 (PSA) and GAPDH. H_2O and $-RT$ controls were negative (data not shown).

subunit in a proteomics analysis of serum from patients with PCa. Abnormal gene expression of proteasome subunits has been reported in several cancer types (29, 32). High plasma proteasome levels reflect the dysregulation of protein synthesis and degradation in cancer cells in contrast to normal cells in which the proteasome complex plays a crucial role in controlling essential cellular functions such as transcription, stress response, cell cycle regulation, cellular differentiation, and DNA repair (33). This is also illustrated by the fact that in malignancies proteasome inhibitors induce apoptosis, have *in vivo* antitumor efficacy, and sensitize malignant cells for conventional therapies (33).

The secretion mechanism of circulating proteasomes in cancer patients and healthy donors is still unknown. Elevated proteasome concentrations in culture media of human leukemic cell lines have been reported, suggesting a proteasome secretion mechanism by tumor cells (34). In this study, we have shown, using native gel electrophoresis and sandwich ELISA of sera from xenografted and control male mice, that at least part of the circulating proteasome subunits are present as proteasome complexes. This is in line with the observation that circulating proteasomes are intact and enzymatically active in plasma from healthy donors and patients with autoimmune disease or leukemia (35, 36).

About half of the tumor-derived proteins circulating in the xenograft-bearing mice, including proteasome subunits, are not secreted proteins but are annotated as being cytoplasmic. One possible explanation for their presence could be the occurrence of necrosis or apoptosis in the xenografts, a well known characteristic of most cancers. Although we did not find evidence for necrosis in the xenografts used for this study, protein secretion via cell death cannot be excluded. Microarray expression data of the identified cytoplasmic proteins showed that these indeed corresponded to genes that are highly expressed in PCa. However, none of the proteins of the 100 most highly expressed genes in PCa (such as ribosomal and cytoskeletal genes) have been identified in the circulation of the xenograft-bearing mice (data not shown). One would expect to detected the proteins of these highly

expressed genes if these are the result of tumor apoptosis. Although this does not rule out the contribution of apoptosis or necrosis, this points toward certain specific processes responsible for the secretion of cytoplasmic proteins.

We hypothesized that one such specific process could be the secretion of proteins via exosomes. A literature search revealed that 13 of the 44 (30%) identified proteins in the xenograft model had earlier been identified in exosomes among which was also the β3 subunit of the proteasome (Table I). First, we showed that the human PCa cell line PC346C is indeed capable of the secretion of exosomes (Fig. 4a). Second, LTQ-FT-ICR-MS/MS and Western blotting analyses of isolated exosomes showed the presence of mainly cytoplasmic proteins, including GAPDH, fructose-bisphosphate aldolase A, ENO1, lactate dehydrogenase B, 14-3-3 protein θ, and proteasome subunits (see Table II and Fig. 5a). Also the exosomal marker CD9 and several proteins up-regulated in PCa, among which was FOLH1, were identified. In addition RAB5A, RAB11A, and HRS, proteins involved in vesicular and endosomal trafficking, were present in the exosome fraction as shown by Western blotting (Fig. 5a). The detection of HRS by Western blotting confirmed the identification of HRS by LTQ-FT-ICR-MS/MS at a setting of one peptide per protein (data not shown).

To argue against the fact that the proteasome signal in the exosome fraction was the result of simultaneous pelleting of exosomes and proteasome complexes, exosomes were further purified by immunoaffinity precipitation utilizing anti-CD9 antibody-coated magnetic beads. This strengthened our finding that proteasomes are present inside exosomes and/or tightly associated with exosomal membranes or external macromolecules. Our observation is in agreement with Almeida *et al.* (37) and Dong *et al.* (38) who showed the presence of proteasomes in late endosomes from which exosomes are formed by invagination and budding. To our knowledge, the present study is the first to describe a specific clearance mechanism for proteasome subunits in cancer cells, providing a possible explanation for the increased proteasome serum levels that have been observed in several types of cancer patients.

An important observation is that PSA was not detectable in the exosome pellets but was abundant in the supernatant. This means that we experimentally separated protein secretion via two different secretion pathways: (i) the typical secretion of signal peptide-containing proteins via the rough endoplasmic reticulum and Golgi apparatus secretory pathway and (ii) the multivesicular body-exosome secretion route. This is in line with our observation that of a total of 48 proteins identified in the exosome fraction the majority are annotated as cytoplasmic whereas only two proteins are annotated as secreted according to the Gene Ontology database. In contrast, 10 of 44 tumor-derived proteins identified in the serum of xenograft-bearing mice are annotated as secreted proteins (Tables I and II). Thus, it seems that several of the cytoplasmic

proteins, including proteasome subunits, present in xenograft sera are at least partly secreted via the exosome pathway in contrast with proteins such as PSA that are typically secreted via the Golgi consecutive secretory pathway.

The putative *in vivo* analogues of exosomes could be prostasomes, secreted vesicles in human seminal fluid, secreted by epithelial prostate cells. Proteomics analysis of human prostasomes revealed 139 proteins, showing a small overlap (7 of 139) with the proteins identified in exosomes in the present study. Among the proteins identified in prostasomes were several glycolysis-related enzymes, heat-shock proteins, and proteins of the annexin family (39). In contrast, no proteasome subunits or members of the tetraspanin family were identified in prostasomes isolated from seminal fluid.

It was recently reported by Valadi *et al.* (16) that exosomes not only contain proteins but also mRNAs, suggesting a potential novel mechanism of genetic exchange between cells. By RNase and trypsin treatment of the isolated exosomes it was confirmed that the mRNA was indeed confined within exosomes and not on external structures or macromolecules. This prompted us to isolate exosomal RNA from the PC346C and VCaP cell lines. Of these cell lines it has been shown that the VCaP cell line expresses the *TMPRSS2-ERG* fusion gene, whereas PC346C does not (27, 28). RT-PCR analysis correctly showed that the PCa-specific *TMPRSS2-ERG* fusion gene is present in exosomal RNA from the VCaP cell line whereas it is absent in exosomal RNA from the PC346C cell line. As it has been reported that exosomes exist in human serum, prostate-specific proteins present in the membrane of exosomes, such as FOLH1, could be used to isolate prostate-specific exosomes to discover and validate new markers for PCa (40). For example, this could lead to the development of a serum test for RNA transcribed from the *TMPRSS2-ERG* gene fusion.

The specific role of exosomes in cancer is still not fully understood, and involvement in processes such as cell-cell communication and antigen representation have been suggested (14–16). The content of exosomes may represent a fingerprint of the cytoplasm of the cancer cell and may establish a unique environment that allows for the occurrence of specific processes. For example, Stoeck *et al.* (41) showed that exosomes may be a platform for ectodomain shedding of transmembrane proteins. In the present study, the presence of a distinct 30-kDa ENO1 band specifically present in the exosome fraction may point toward the occurrence of unique proteolytic activity inside exosomes (Fig. 5a). It has recently been suggested that exosomes secreted from cancer cells support immune escape as well as tumor growth (15). Also exosomes have been reported to induce angiogenesis and to transfer metastatic activity from highly to poorly metastatic tumor cells (42). Of the proteins identified in the exosomes in the present study, CD151 and the metalloproteinases ADAM10 and ADAM15 have been linked to tumor invasive-

ness and prognosis (43–45). The proteasomes identified in exosomes may harbor a similar function.

In conclusion, the present study shows that, although their function is unclear, exosomes offer unique possibilities for PCa biomarker discovery as they give insight information about the interior of the cancer cell both on the protein and RNA levels. Future studies will focus on the validation of several identified exosomal proteins as well as on the detection of exosomal RNA, including the *TMPRSS2-ERG* and other gene fusion transcripts in exosomes isolated from patient populations, to establish new biomarkers for PCa diagnosis and prognosis.

** To whom correspondence should be addressed: Dept. of Urology, Josephine Nefkens Inst., Erasmus MC, Rm. Be362a, P. O. Box 2040, 3000 CA Rotterdam, The Netherlands. Tel.: 31-10-704-3672; Fax: 31-10-704-4661; E-mail: g.jenster@erasmusmc.nl.

REFERENCES

1. Stamey, T. A., Yang, N., Hay, A. R., McNeal, J. E., Freiha, F. S., and Redwine, E. (1987) Prostate-specific antigen as a serum marker for adenocarcinoma of the prostate. *N. Engl. J. Med.* **317,** 909–916
2. McDavid, K., Lee, J., Fulton, J. P., Tonita, J., and Thompson, T. D. (2004) Prostate cancer incidence and mortality rates and trends in the United States and Canada. *Public Health Rep.* **119,** 174–186
3. Thompson, I. M., Pauler, D. K., Goodman, P. J., Tangen, C. M., Lucia, M. S., Parnes, H. L., Minasian, L. M., Ford, L. G., Lippman, S. M., Crawford, E. D., Crowley, J. J., and Coltman, C. A., Jr. (2004) Prevalence of prostate cancer among men with a prostate-specific antigen level < or =4.0 ng per milliliter. *N. Engl. J. Med.* **350,** 2239–2246
4. Mikolajczyk, S. D., and Rittenhouse, H. G. (2004) Tumor-associated forms of prostate specific antigen improve the discrimination of prostate cancer from benign disease. *Rinsho Byori* **52,** 223–230
5. Paul, B., Dhir, R., Landsittel, D., Hitchens, M. R., and Getzenberg, R. H. (2005) Detection of prostate cancer with a blood-based assay for early prostate cancer antigen. *Cancer Res.* **65,** 4097–4100
6. Reiter, R. E., Gu, Z., Watabe, T., Thomas, G., Szigeti, K., Davis, E., Wahl, M., Nisitani, S., Yamashiro, J., Le Beau, M. M., Loda, M., and Witte, O. N. (1998) Prostate stem cell antigen: a cell surface marker overexpressed in prostate cancer. *Proc. Natl. Acad. Sci. U. S. A.* **95,** 1735–1740
7. Rubin, M. A., Zhou, M., Dhanasekaran, S. M., Varambally, S., Barrette, T. R., Sanda, M. G., Pienta, K. J., Ghosh, D., and Chinnaiyan, A. M. (2002) α-Methylacyl coenzyme A racemase as a tissue biomarker for prostate cancer. *J. Am. Med. Assoc.* **287,** 1662–1670
8. Stephan, C., Jung, K., Lein, M., Sinha, P., Schnorr, D., and Loening, S. A. (2000) Molecular forms of prostate-specific antigen and human kallikrein 2 as promising tools for early diagnosis of prostate cancer. *Cancer Epidemiol. Biomark. Prev.* **9,** 1133–1147
9. de Kok, J. B., Verhaegh, G. W., Roelofs, R. W., Hessels, D., Kiemeney, L. A., Aalders, T. W., Swinkels, D. W., and Schalken, J. A. (2002) DD3(PCA3), a very sensitive and specific marker to detect prostate tumors. *Cancer Res.* **62,** 2695–2698
10. Kumar-Sinha, C., Tomlins, S. A., and Chinnaiyan, A. M. (2008) Recurrent gene fusions in prostate cancer. *Nat. Rev. Cancer* **8,** 497–511
11. van Weerden, W. M., de Ridder, C. M., Verdaasdonk, C. L., Romijn, J. C., van der Kwast, T. H., Schroder, F. H., and van Steenbrugge, G. J. (1996) Development of seven new human prostate tumor xenograft models and their histopathological characterization. *Am. J. Pathol.* **149,** 1055–1062
12. van den Bemd, G. J., Krijgsveld, J., Luider, T. M., van Rijswijk, A. L., Demmers, J. A., and Jenster, G. (2006) Mass spectrometric identification of human prostate cancer-derived proteins in serum of xenograft-bearing mice. *Mol. Cell. Proteomics* **5,** 1830–1839
13. Omenn, G. S., States, D. J., Adamski, M., Blackwell, T. W., Menon, R., Hermjakob, H., Apweiler, R., Haab, B. B., Simpson, R. J., Eddes, J. S., Kapp, E. A., Moritz, R. L., Chan, D. W., Rai, A. J., Admon, A., Aebersold, R., Eng, J., Hancock, W. S., Hefta, S. A., Meyer, H., Paik, Y. K., Yoo, J. S., Ping, P., Pounds, J., Adkins, J., Qian, X., Wang, R., Wasinger, V., Wu, C. Y., Zhao, X., Zeng, R., Archakov, A., Tsugita, A., Beer, I., Pandey, A., Pisano, M., Andrews, P., Tammen, H., Speicher, D. W., and Hanash, S. M. (2005) Overview of the HUPO Plasma Proteome Project: results from the pilot phase with 35 collaborating laboratories and multiple analytical groups, generating a core dataset of 3020 proteins and a publicly-available database. *Proteomics* **5,** 3226–3245
14. Thery, C., Zitvogel, L., and Amigorena, S. (2002) Exosomes: composition, biogenesis and function. *Nat. Rev. Immunol.* **2,** 569–579
15. Valenti, R., Huber, V., Iero, M., Filipazzi, P., Parmiani, G., and Rivoltini, L. (2007) Tumor-released microvesicles as vehicles of immunosuppression. *Cancer Res.* **67,** 2912–2915
16. Valadi, H., Ekstrom, K., Bossios, A., Sjostrand, M., Lee, J. J., and Lotvall, J. O. (2007) Exosome-mediated transfer of mRNAs and microRNAs is a novel mechanism of genetic exchange between cells. *Nat. Cell Biol.* **9,** 654–659
17. Marques, R. B., van Weerden, W. M., Erkens-Schulze, S., de Ridder, C. M., Bangma, C. H., Trapman, J., and Jenster, G. (2006) The human PC346 xenograft and cell line panel: a model system for prostate cancer progression. *Eur. Urol.* **49,** 245–257
18. Keller, A., Nesvizhskii, A. I., Kolker, E., and Aebersold, R. (2002) Empirical statistical model to estimate the accuracy of peptide identifications made by MS/MS and database search. *Anal. Chem.* **74,** 5383–5392
19. Nesvizhskii, A. I., Keller, A., Kolker, E., and Aebersold, R. (2003) A statistical model for identifying proteins by tandem mass spectrometry. *Anal. Chem.* **75,** 4646–4658
20. Baumeister, W., Walz, J., Zuhl, F., and Seemuller, E. (1998) The proteasome: paradigm of a self-compartmentalizing protease. *Cell* **92,** 367–380
21. Elsasser, S., Schmidt, M., and Finley, D. (2005) Characterization of the proteasome using native gel electrophoresis. *Methods Enzymol.* **398,** 353–363
22. Dutaud, D., Aubry, L., Henry, L., Levieux, D., Hendil, K. B., Kuehn, L., Bureau, J. P., and Ouali, A. (2002) Development and evaluation of a sandwich ELISA for quantification of the 20S proteasome in human plasma. *J. Immunol. Methods* **260,** 183–193
23. Marques, R. B., Erkens-Schulze, S., de Ridder, C. M., Hermans, K. G., Waltering, K., Visakorpi, T., Trapman, J., Romijn, J. C., van Weerden, W. M., and Jenster, G. (2005) Androgen receptor modifications in prostate cancer cells upon long-term androgen ablation and antiandrogen treatment. *Int. J. Cancer* **117,** 221–229
24. Hegmans, J. P., Bard, M. P., Hemmes, A., Luider, T. M., Kleijmeer, M. J., Prins, J. B., Zitvogel, L., Burgers, S. A., Hoogsteden, H. C., and Lambrecht, B. N. (2004) Proteomic analysis of exosomes secreted by human mesothelioma cells. *Am. J. Pathol.* **164,** 1807–1815
25. Mortz, E., Krogh, T. N., Vorum, H., and Gorg, A. (2001) Improved silver staining protocols for high sensitivity protein identification using matrix-assisted laser desorption/ionization-time of flight analysis. *Proteomics* **1,** 1359–1363
26. Claverol, S., Burlet-Schiltz, O., Girbal-Neuhauser, E., Gairin, J. E., and Monsarrat, B. (2002) Mapping and structural dissection of human 20 S proteasome using proteomic approaches. *Mol. Cell. Proteomics* **1,** 567–578
27. Hermans, K. G., van Marion, R., van Dekken, H., Jenster, G., van Weerden, W. M., and Trapman, J. (2006) TMPRSS2:ERG fusion by translocation or interstitial deletion is highly relevant in androgen-dependent prostate cancer, but is bypassed in late-stage androgen receptor-negative pros-

tate cancer. *Cancer Res.* **66,** 10658–10663

28. Tomlins, S. A., Rhodes, D. R., Perner, S., Dhanasekaran, S. M., Mehra, R., Sun, X. W., Varambally, S., Cao, X., Tchinda, J., Kuefer, R., Lee, C., Montie, J. E., Shah, R. B., Pienta, K. J., Rubin, M. A., and Chinnaiyan, A. M. (2005) Recurrent fusion of TMPRSS2 and ETS transcription factor genes in prostate cancer. *Science* **310,** 644–648

29. Kumatori, A., Tanaka, K., Inamura, N., Sone, S., Ogura, T., Matsumoto, T., Tachikawa, T., Shin, S., and Ichihara, A. (1990) Abnormally high expression of proteasomes in human leukemic cells. *Proc. Natl. Acad. Sci. U. S. A.* **87,** 7071–7075

30. Milano, A., Iaffaioli, R. V., and Caponigro, F. (2007) The proteasome: a worthwhile target for the treatment of solid tumours? *Eur. J. Cancer* **43,** 1125–1133

31. Byrne, J. C., Downes, M. R., O'Donoghue, N., O'Keane, C., O'Neill, A., Fan, Y., Fitzpatrick, J. M., Dunn, M. J., and Watson, R. W. (2009) 2D-DIGE as a strategy to identify serum markers for the progression of prostate cancer. *J. Proteome Res.* **8,** 942–957

32. Kanayama, H., Tanaka, K., Aki, M., Kagawa, S., Miyaji, H., Satoh, M., Okada, F., Sato, S., Shimbara, N., and Ichihara, A. (1991) Changes in expressions of proteasome and ubiquitin genes in human renal cancer cells. *Cancer Res.* **51,** 6677–6685

33. Voorhees, P. M., Dees, E. C., O'Neil, B., and Orlowski, R. Z. (2003) The proteasome as a target for cancer therapy. *Clin. Cancer Res.* **9,** 6316–6325

34. Wada, M., Kosaka, M., Saito, S., Sano, T., Tanaka, K., and Ichihara, A. (1993) Serum concentration and localization in tumor cells of proteasomes in patients with hematologic malignancy and their pathophysiologic significance. *J. Lab. Clin. Med.* **121,** 215–223

35. Ma, W., Kantarjian, H., O'Brien, S., Jilani, I., Zhang, X., Estrov, Z., Ferrajoli, A., Keating, M., Giles, F., and Albitar, M. (2008) Enzymatic activity of circulating proteasomes correlates with clinical behavior in patients with chronic lymphocytic leukemia. *Cancer* **112,** 1306–1312

36. Zoeger, A., Blau, M., Egerer, K., Feist, E., and Dahlmann, B. (2006) Circu-lating proteasomes are functional and have a subtype pattern distinct from 20S proteasomes in major blood cells. *Clin Chem.* **52,** 2079–2086

37. Almeida, C. G., Takahashi, R. H., and Gouras, G. K. (2006) β-Amyloid accumulation impairs multivesicular body sorting by inhibiting the ubiquitin-proteasome system. *J. Neurosci.* **26,** 4277–4288

38. Dong, J., Chen, W., Welford, A., and Wandinger-Ness, A. (2004) The proteasome α-subunit XAPC7 interacts specifically with Rab7 and late endosomes. *J. Biol. Chem.* **279,** 21334–21342

39. Utleg, A. G., Yi, E. C., Xie, T., Shannon, P., White, J. T., Goodlett, D. R., Hood, L., and Lin, B. (2003) Proteomic analysis of human prostasomes. *Prostate* **56,** 150–161

40. Caby, M. P., Lankar, D., Vincendeau-Scherrer, C., Raposo, G., and Bonnerot, C. (2005) Exosomal-like vesicles are present in human blood plasma. *Int. Immunol.* **17,** 879–887

41. Stoeck, A., Keller, S., Riedle, S., Sanderson, M. P., Runz, S., Le Naour, F., Gutwein, P., Ludwig, A., Rubinstein, E., and Altevogt, P. (2006) A role for exosomes in the constitutive and stimulus-induced ectodomain cleavage of L1 and CD44. *Biochem. J.* **393,** 609–618

42. Hao, S., Ye, Z., Li, F., Meng, Q., Qureshi, M., Yang, J., and Xiang, J. (2006) Epigenetic transfer of metastatic activity by uptake of highly metastatic B16 melanoma cell-released exosomes. *Exp. Oncol.* **28,** 126–131

43. Ginestra, A., La Placa, M. D., Saladino, F., Cassara, D., Nagase, H., and Vittorelli, M. L. (1998) The amount and proteolytic content of vesicles shed by human cancer cell lines correlates with their in vitro invasiveness. *Anticancer Res.* **18,** 3433–3437

44. Hashida, H., Takabayashi, A., Tokuhara, T., Hattori, N., Taki, T., Hasegawa, H., Satoh, S., Kobayashi, N., Yamaoka, Y., and Miyake, M. (2003) Clinical significance of transmembrane 4 superfamily in colon cancer. *Br. J. Cancer* **89,** 158–167

45. Kuefer, R., Day, K. C., Kleer, C. G., Sabel, M. S., Hofer, M. D., Varambally, S., Zorn, C. S., Chinnaiyan, A. M., Rubin, M. A., and Day, M. L. (2006) ADAM15 disintegrin is associated with aggressive prostate and breast cancer disease. *Neoplasia* **8,** 319–329